http://dx.doi.org/10.5012/bkcs.2014.35.3.949

Structural Transformation and Gas Adsorption Properties of Interpenetrated IRMOF-8†

Jang-Hoon Cho, Sang Moon Lee,‡ Jong Won Shin, Dohyun Moon,§ Kil Sik Min, Myoung Soo Lah,# and Hong-In Lee*

Department of Chemistry and Green-Nano Materials Research Center, Kyungpook National University, Daegu 702-701, Korea
**E-mail: leehi@knu.ac.kr*
‡Division of Materials Science, Korea Basic Science Institute, Daejeon 305-333, Korea
§Pohang Accelerator Laboratory, Pohang, Kyungbook 790-784, Korea
#Interdisciplinary School of Green Energy, Ulsan National Institute of Science and Technology, Ulsan 689-798, Korea
Received September 23, 2013, Accepted September 30, 2013

Key Words : MOF, Gas adsorption, Crystal structure

Metal-organic frameworks (MOFs) have been intensively developed and investigated for their huge potential in gas storage, separation, clean energy, catalysis, and many others.[1-7] One of the early successes in developing MOFs is IRMOF-8 (isoreticular MOF-8) whose network can be viewed as an assembly of cubes.[8-10] Since IRMOF-8 was reported, its properties have been intensively studied. During the years of investigating IRMOF-8, it has been noticed that the observed surface area of bulk IRMOF-8 seemed much smaller than the calculated value, leading the propose of an interpenetrated IRMOF-8.[10,11] It was very recent that the synthesis and structure of the interpenetrated IRMOF-8 was reported and its gas-adsorption and photoluminescence properties were explored.[12,13] Interestingly, the CO_2 uptake of the interpenetrated IRMOF-8 (SUMOF-3) was greatly enhanced, compared to that of the original IRMOF-8, at pressures relevant for capturing CO_2 without compressing flue gases.[12] In this study, we have developed an interpenetrated IRMOF-8 using deferent synthetic methods from the previous ones to explore its structural characteristics and gas absorption abilities.

Two kinds of the interpenetrated IRMOF-8 were solvothermally synthesized and crystallized in two different solvent systems: INT-IRMOF-8-A in the mixture solvent of *N,N'*-dimethylformamide (DMF) and 1,4-dioxane, INT-IRMOF-8-B in the mixture solvent of DMF and formic acid.

INT-IRMOF-8-A is crystallographically analyzed to be found as the two-fold interpenetrated analogue of IRMOF-8. Each of the two identical, interpenetrated, networks is constructed by Zn_4O clusters and 2,6-naphthalenedicarboxylate (NDC) linkers with the **pcu** topology. The oxygen atom of the Zn_4O cluster lies at the center of the cluster with the tetrahedral coordination of four Zn atoms. (Figure 1(a)) Each cluster is coordinated by DMF, water, and six NDCs, which are working as the linkers to form the network (Figure 1(b)). The carboxylate oxygen atoms of NDC bridge two Zn atoms of the cluster *via* μ_2-η^1: η^1 mode. Two types of Zn coordination structures are found. One is a tetrahedral ZnO_4 and the other is an octahedral ZnO_6. Three Zn atoms of the cluster take ZnO_4 tetrahedral coordination and the remaining one Zn atom takes ZnO_6 octahedral coordination. The oxygen atoms are from the NDC linker in the ZnO_4 coordination, and additional two oxygen atoms are from DMF and water molecules in ZnO_6.

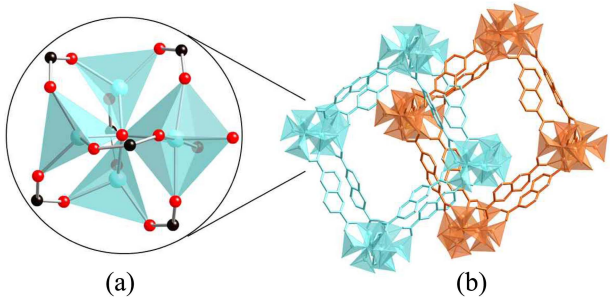

Figure 1. Structures of (a) Zn_4O core and (b) the interpenetrated rhombohedra constituting the interpenetrated 3D network of INT-IRMOF-8-A.[14] In (a), the red, black, and sky-blue spheres represent oxygen, zinc, and carbon atoms, respectively. Polyhedrons denote the coordination geometries of Zn atoms.

The crystal structure of INT-IRMOF-8-B is basically same as that of INT-IRMOF-8-A, but the deviation from the average angles of the rhombohedron in INT-IRMOF-8-B is wider than in INT-IRMOF-8-A. Because the lengths of the edges are determined by NCD, there is no noticeable difference found in the edge lengths. These structures are similar to the previously reported interpenetrated IRMOF-8 (SUMOF-3). The dimensions of the rhombohedra of both the crystals are compared in Table 1. The structural similarities in INT-IRMOF-8-A, INT-IRMOF-8-B, and SUMOF-3 are also found in the simulated powder X-ray diffraction (PXRD) patterns (Figure 2).

The structural transformations of INT-IRMOF-8-A were explored by removing the guest molecules (activating the material) and by exchanging the ligand solvent molecules, respectively. Figure 2 compares the PXRD patterns of the activated with the as-synthesized forms of INT-IRMOF-8-A. The PXRD pattern of the as-synthesized INT-IRMOF-8-A

†This paper is to commemorate Professor Myung Soo Kim's honourable retirement.

Table 1. Comparison of rhombohedra constituting the frameworks of interpenetrated IRMOF-8s

Crystals	Angles (°)	Lengths (Å)[e]
INT-IRMOF-8-A[a]	79.6, 86.9, 86.9[d]	15.0
	79.6, 83.8, 84.2[d]	
INT-IRMOF-8-B[a]	73.8, 83.3, 88.0	15.0
INT-IRMOF-8-C[a]	80.1, 81.9, 84.0	15.0
SUMOF-3[b]	76.5, 84.3, 87.5	15.0
IRMOF-8[c]	90.0, 90.0, 90.0	15.0

[a]This work. [b]Ref 12. [c]Ref 10. [d]Two rhombohedra are alternatively stacked. [e]Distances between the two central O atoms of ZnO_4 clusters.

closely resembles the simulated pattern, indicating that the bulk sample contains mostly INT-IRMOF-8-A. After activating the sample at 400 °C, it exhibits vastly different PXRD from the original. The PXRD pattern of the activated INT-IRMOF-8-A is simpler than that of the as-synthesized, implying that the framework of INT-IRMOF-8-A is flexible and that the activated INT-IRMOF-8-A seems to achieve a trigonal trapezohedron-like framework.

A similar structural transformation was also observed by exchanging ligand solvent molecules. After the crystals of INT-IRMOF-8-A were immersed in ethanol for 3 days, the crystals were collected to be dried. The resulting single crystal (INT-IRMOF-8-C) was analyzed by X-ray diffraction. The crystal structure of INT-IRMOF-8-C shows the same interpenetrated networks constructed by Zn_4O clusters and NDC linkers as those of INT-IRMOF-8-A and INT-IRMOF-8-B. The ligand DMF molecules found in INT-IRMOF-8-A and INT-IRMOF-8-B is replaced with water in INT-IRMOF-8-C. The rhombohedron constituting the framework of INT-IRMOF-8-C has less deviation from the average angle than other interpenetrated IRMOF-8s as listed in Table 1. Therefore, the rhombohedron of INT-IRMOF-8-C is

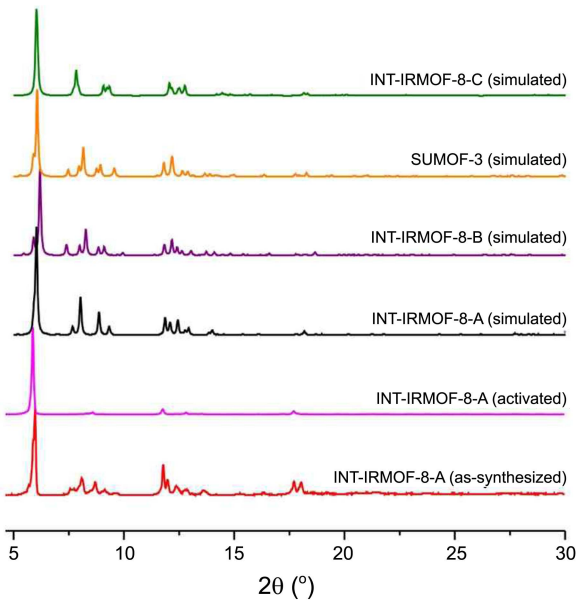

Figure 2. Experimental and simulated PXRD patterns of the interpenetrated IRMOF-8s.

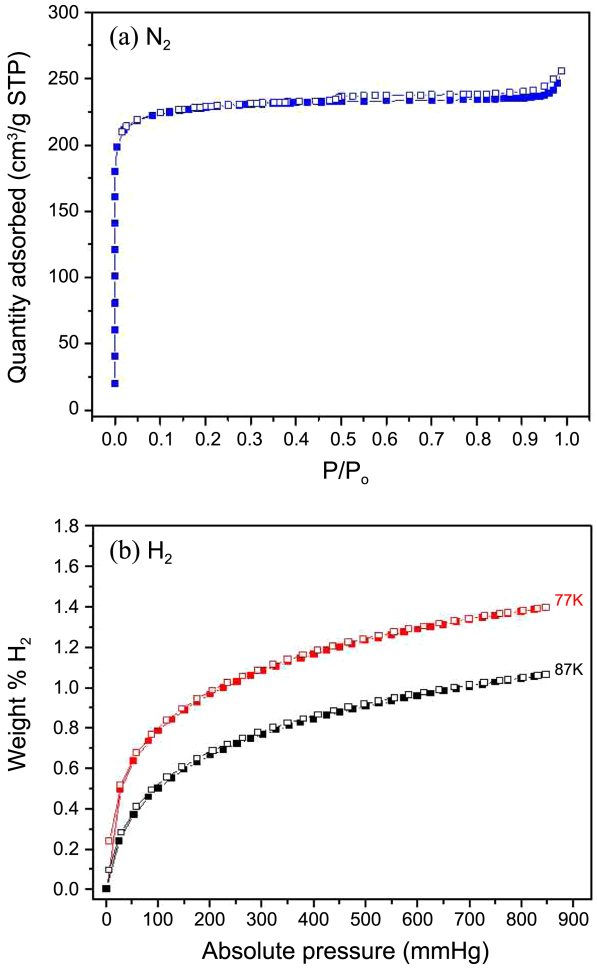

Figure 3. Adsorption isotherms of (a) N_2 and (b) H_2. Filled and open squares represent the adsorption and desorption isotherms, respectively. For N_2, P_o = 760 torr.

closer to trigonal trapezohedron than those of other interpenetrated IRMOF-8.

The structural transformations of INT-IRMOF-8-A found both by removing guest molecules and by exchanging the ligand solvent molecules suggest that the framework of the interpenetrated IRMOF-8 is flexible and the detailed geometric structure of the framework is determined by the ligand solvent molecules. It is likely that the rhombohedron tends to form a trigonal trapezohedron shape not cube upon removing both the guest and ligand molecules because of the π-π interaction between the two interpenetrated frameworks.

Thermal stability of the INT-IRMOF-8-A was tested with thermogravimetric analysis (TGA). Figure S1 shows the TGA curve of INT-IRMOF-8-A. The interpenetrated IRMOF-8 loses all its coordinated solvents and guest molecules at 200 °C and starts to decompose at 430 °C. Decomposition process ends at 515 °C and slowly loses its mass at higher temperature under N_2.

As found in Figure S1, INT-IRMOF-8-A loses its solvent and guest molecules upon activation to generate porosity. This porosity can be used for gas storage and separation. Porosity of INT-IRMOF-8-A was measured by using N_2

Table 2. Porosities of INT-IRMOF-8-A and IRMOF-8

Sample	INT-IRMOF-8-A[a]	IRMOF-8
BET surface area (m^2/g)	887	2110[d,e]
Micropore volume (cm^3/g)[b]	0.329	0.551[d,f]
Pore volume (cm^3/g)[c]	0.353	0.693[d,f]
Mean pore diameter (nm)[c]	1.02	1.23[g]

[a]This work. [b]*t*-plot analysis. [c]H-K analysis. [d]The highest values among the reported values. [e]Ref. 15. [f]Ref. 16. [g]Ref. 17.

physisorption at 77 K. Figure 3(a) shows the N_2 adsorption-desorption isotherm obtained from the sample after chloroform exchange and degassing under vacuum for 6 h at 100 °C. The plot shows a reversible type-I isotherm revealing the microporous INT-IRMOF-8-A, and the specific BET surface area is derived to be 888 m^2/g from the isotherm. Table 2 compares the porosities of INT-IRMO-8-A and IRMOF-8. The mean pore diameter is smaller in INT-IRMOF-8-A than in IRMOF-8. This could be explained by the decrease of the mircopore sizes originated from the interpenetrated frameworks in INT-IRMOF-8-A. The specific BET surface area and pore volume are smaller than the highest reported values of IRMOF-8.

The H_2 adsorption characteristics of INT-IRMOF-8 at 77 K and 88 K are displayed in Figure 3(b). The H_2 adsorption-desorption curve again shows a reversible type-I isotherm characteristics as found for N_2. The H_2 uptake of 1.38 wt % at 77 K and 1 atm is almost the same as IRMOF-8.[17,18] Both the H_2 isotherms measured at 77 K and 88 K are not saturated in the range of 0-1 atm. Therefore, it is expected that INT-IRMOF-8-A can store more quantity of H_2 at higher pressure.

In summary, we have solvothermally synthesized two kinds of the interpenetrated IRMOF-8 in two different solvent systems: INT-IRMOF-8-A and INT-IRMOF-8-B. X-ray crystallographic analyses showed that both MOFs were the two-fold interpenetrated analogue of IRMOF-8 with **pcu** topology. The shape of the hexahedron constituting the **pcu** topology is a rhombohedron in the penetrated IRMOF-8s, which differs from a cube in IRMOF-8. When the ligand solvent molecules of INT-IRMOF-8-A were replaced with H_2O molecules (INT-IRMOF-8-C), the rhombohedron constituting the framework of INT-IRMOF-8-C had less deviation from the average angle than other interpenetrated IRMOF-8s, so that the rhombohedron of INT-IRMOF-8-C was closer to trigonal trapezohedron than those of other interpenetrated IRMOF-8s. This kind of trend was also found when the solvent and guest molecules were removed. It is likely that the rhombohedron tends to form a trigonal trapezohedron shape not cube upon removing both the guest and ligand molecules because of the π-π interaction between the two interpenetrated frameworks. The gas adsorption capacity of INT-IRMOF-8-A was examined using N_2 and H_2 isotherms. INT-IRMOF-8-A was found to be a type-I microporous material. And INT-IRMOF-8-A has smaller specific BET surface area and similar H_2 uptake capacity, compared with IRMOF-8.

Experimental

Synthesis. INT-IRMOF-8-A was synthesized solvothermally. $Zn(NO_3)_2{\cdot}6H_2O$ (0.17 g, 0.57 mmol) and 2,6-naphthalenedicarboxylic acid (H_2NDC, 0.06 g, 0.28 mmol) were dissolved in a mixed solvent of DMF (10 mL) and 1,4-dioxane (2 mL) and stirred for 2 h at room temperature. The resulting solution was sealed in a teflon-capped scintillation vial for 24 h at 110 °C. Colorless crystals were filtered to be collected and washed three times with a mixed solvent of DMF and 1,4-dioxane. The crystals were dried in vacuum evaporator for 2 h. Yield: 95%. The chemical formula for the activated INT-IRMOF-8-A is $Zn_4O(NDC)_3$, as derived from the structural refinement and elemental analysis. Calculated (%): C 47.00, H 1.97, N 0.0. Found (%): C 46.45, H 1.84, N 0.0. INT-IRMOF-8-B was synthesized similarly in a mixed solvent of DMF (12 mL) and formic acid (100 mL).

INT-IRMOF-8-C was obtained from INT-IRMOF-8-A. INT-IRMOF-8-A was placed in ethanol solvent at room temperature for 3 days and dried in vacuum for 2 h. Colorless crystals were collected for single crystal analysis.

Physical Measurements. Elemental analysis (EA) was performed using a Perkin-Elmer 2400 CHN analyzer. Thermogravimetric analysis (TGA) was performed on a Seiko TG/DTA 320. The samples were heated from 30 to 800 °C with 10 °C/min scan speed under N_2 flow. Powder X-ray diffraction (PXRD) data were measured on a Shimadzu XRD 600 using Cu $K_{\alpha1}$ radiation (λ = 1.5418 Å). The numerical PXRD simulations were performed using Mercury 3.1 software. N_2 and H_2 adsorption–desorption isotherms were collected at 77 K and/or 88 K with a standard static volumetric technique on a Micromeritics ASAP2010 analyzer. The isotherms of the MOFs were recorded after chloroform exchange and degassing under vacuum for 6 h at 100 °C.

X-ray Crystallography. X-ray diffraction data for INT-IRMOF-8-A and INT-IRMOF-8-C were collected on a 4AMXW ADSC Quantum-210 detector with a Pt-coated Si double crystal monochromator (λ = 0.77000 Å for INT-IRMOF-8-A and λ = 0.90000 Å for INT-IRMOF-8-C) at 100(2) K in Pohang Accelerator Laboratory (PAL), Korea. X-ray diffraction data for INT-IRMOF-8-B were collected on a Bruker SMART APEXII diffractometer equipped with graphite monochromated MoK_α radiation (λ = 0.71073 Å) at 200(2) K in Korea Basic Science Institute. The crystal structures were solved by the direct method and refined by full-matrix least-squares calculation with the SHELXTL software package.[19] The positions of all non-hydrogen atoms were refined with anisotropic displacement factors. However, due to the disorder, carbon atom (C24) of the 2,6-naphthalenedicarboxylate (NDC) anion was refined isotropically in INT-IRMOF-8-B. All hydrogen atoms were theoretically added and included in the final refinement. The final refinement was performed with modification of the structure factors for contribution of the disordered solvent electron densities using the PLATON/SQUEEZE program.[20] Crystal data and structure refinements are listed in table S1. Crystallographic data for the structures reported in this paper have been

deposited with Cambridge Crystallographic Data Centre (Deposition No. CCDC-957268 for INT-IRMOF-8-A, CCDC-957270 for INT-IRMOF-8-B, and CCDC-957269 for INT-IRMOF-8-C). These data can be obtained free of charge from the Cambridge Crystallographic Data Centre *via* http://www.ccdc.cam.ac.uk/conts/retrieving.html

Acknowledgments. This research was supported by Basic Science Research Program through the National Research Foundation of Korea (NRF) funded by the Ministry of Education, Science and Technology (2013-053145).

Supporting Information. Thermogravimetric analysis data, crystal data and structure refinements are included in supporting information.

References and Note

1. Stock, N.; Biswas, N. *Chem. Rev.* **2012**, *112*, 933-969.
2. Wang, C.; Zhang, T.; Lin, W. *Chem. Rev.* **2012**, *112*, 1084-1104.
3. Li, J.-R.; Sculley, J.; Zhou, H.-C. *Chem. Rev.* **2012**, *112*, 869-932.
4. Kreno, J. E.; Leong, K.; Farha, O. K.; Allendorf, M.; Van Duyne, R. P.; Hupp, J. T. *Chem. Rev.* **2012**, *112*, 1105-1125.
5. Suh, M. P.; Park, H. J.; Prasad, T. K.; Lim, D.-W. *Chem. Rev.* **2012**, *112*, 782-835.
6. Yaghi, O. M.; O'Keeffe, M. *Chem. Rev.* **2012**, *112*, 675-702.
7. Gu, Z.-Y.; Yang, C.-X.; Chang, N.; Yan, X.-P. *Acc. Chem. Res.* **2012**, *45*, 734-735.
8. Eddaoudi, M.; Kim, J.; Rosi, N.; Vodak, D.; Wachter, J.; O'Keeffe, M.; Yaghi, O. M. *Sicence* **2002**, *295*, 469-472.
9. Rosi, N. L.; Eckert, J.; Eddaoudi, M.; Vodak, D. T.; Kim, J.; O'Keeffe, M.; Yaghi, O. M. *Sicence* **2003**, *300*, 1127-1129.
10. Yaghi, O. M.; Eddaoudi, M.; Li, H.; Kim, J.; Rosi, N. *US Pat.* 6930193 B2, 2005.
11. Siberio-Pérez, D. Y.; Wong-Foy, A. G.; Yaghi, O. M.; Matzger, A. J. *Chem. Mater.* **2007**, *19*, 3681-3685.
12. Yao, Q.; Su, J.; Cheung, O.; Liu, Q.; Hedin, N.; Zou, X. *J. Mater. Chem.* **2012**, *22*, 10345-10351.
13. Perry IV, J. J.; Feng, P. L.; Meek, S. T.; Leong, K.; Doty, F. P.; Allendorf, M. P. *J. Mater. Chem.* **2012**, *22*, 10235-10248.
14. Strictly speaking, half the interpenetrated rhombohedra constitute the whole framework by repeated translational motion along the three edge directions.
15. Nguyen, L. T. L.; Nguyen, C. V.; Dang, G. H.; Le, K. K. A.; Phan, N. T. S. *J. Mol. Cat. A: Chem.* **2011**, *349*, 28-35.
16. Orefuwa, S. A.; Yang, H.; Goudy, A. J. *Micropor. Mesopor. Mater.* **2012**, *153*, 88-93.
17. Rowsell, J. L. C.; Millward, A. R.; Park, K. S.; Yaghi, O. M. *J. Am. Chem. Soc.* **2004**, *126*, 5666-5667.
18. Li, Y.; Yang, R. T. *J. Am. Chem. Soc.* **2006**, *128*, 726-727.
19. Sheldrick, G. M. *SHELXTL-PLUS*, Crystal Structure Analysis Package, Bruker Analytical X-Ray, Madison, WI, USA, 1997.
20. Spek, A. L. *J. Appl. Crystallogr.* **2003**, *36*, 7-13.